Archives of Materials Science and Engineering

Volume 120
Issue 1
March 2023
Pages 22-29

International Scientific Journal
published monthly by the
World Academy of Materials
and Manufacturing Engineering

DOI: 10.5604/01.3001.0053.6014

Numerical modelling of SS316L powder flowability for laser powder-bed fusion

A. Bouabbou*, S. Vaudreuil
Euro-Mediterranean University of Fez, Euromed Polytechnic School (EPS), Fès, Morocco
* Corresponding e-mail address: Abdelkrim.bouabbou@ueuromed.org
ORCID identifier: https://orcid.org/0000-0001-8606-5507 (A.B.)

ABSTRACT

Purpose: This work aims to improve the powder-bed spreading process for laser powder bed fusion additive manufacturing by gaining a greater understanding of metal powder flowability through numerical modelling and in-situ experimentation.

Design/methodology/approach: Using the Discrete Element Method (DEM) to study the flowability of the powder and its intrinsic properties. A high-fidelity particle-scale model was developed to capture the dynamics of metal particle interactions in a virtual Hall flow meter based on a modified Beverloo law. The results are validated experimentally using the Hall flow static powder characterisation technique.

Findings: For SS316L powder alloy with the hall-value of 29s/50g and with an angle of repose (AOR) of 32°, the modelled powder that exhibited the same flow behaviour was found using 0.5 for both rolling and sliding coefficients resulting in simulated Hall value of 28.55s/50g with a simulated flow rate of 0.571 g/s, which is validated by AOR of the simulated powder [31.2°-32.6°]. However, rolling friction had minimal effect on the mass flow rate but increased the angle of repose. Sliding friction significantly decreased the mass flow rate and increased AOR.

Research limitations/implications: DEM is an ideal method to study flowability. However, there are certain constraints imposed on the computational power by a number of simulated particles and simulation time-step. Future research may involve investigating other dynamic flowability characterisation techniques.

Practical implications: Enabling a better understanding of powder particle flow at a micro-scale by modelling powder flowability. This leads to simulating a more realistic powder bed and improving the powder spreading process, leading to better AM parts quality.

Originality/value: This paper provides a unique approach for modelling the flowability of SS316L powder using a Beverloo law-based design of the Hall flow meter. This will improve the modelling of the spreading process needed for metal 3D printing.

Keywords: Discrete element method, Flowability, Hall flow, Metal powder, SS316L, LIGGGHTS

Reference to this paper should be given in the following way:

A. Bouabbou, S. Vaudreuil, Numerical modelling of SS316L powder flowability for laser powder-bed fusion, Archives of Materials Science and Engineering 120/1 (2023) 22-29.

DOI: https://doi.org/10.5604/01.3001.0053.6014

METHODOLOGY OF RESEARCH, ANALYSIS AND MODELLING

1. Introduction

Laser powder bed fusion (LPBF), like any other additive manufacturing (AM) technique, employs the same basic principle to produce high-quality metallic parts. The LPBF procedure begins with slicing a 3D CAD model into thin layers evenly. The physical manufacturing process relies on depositing a thin powder layer spread by a raking or rolling system. This is followed by selectively melting each powder layer using a laser beam (ISO/ASTM: PBF-LB/M). After lowering the build plate, this process is repeated layer by layer until the part is finished. Several aspects influence the quality of the manufactured products, including 3D build parameters, metal powder composition, and powder bed qualities. Powder flowability, packing density, morphology, and particle size distribution affect the powder bed. Each of these features can significantly impact the quality of the manufactured metallic part. A low-quality powder bed, for example, can have negative implications such as melt pool instability, partial melting, and so forth [1].

To obtain higher quality, faster manufacturing, and cheaper costs, it is critical to investigate the effect of different process parameters on the deposited powder layer. This process is made more difficult by the spreading parameters and the variability in the powder quality caused by the various metal powder suppliers, the storage and the recycling conditions. The interest in powder granulometry in AM led many researchers to investigate the impacts of power morphology distribution and density, flowability and thermal properties on the part's density, surface quality, and other mechanical properties – authors like Riener et al. [2] used the Hausner ratio and Avalanche angle from the revolution powder analyser (RPA) as the main metric of metallic powder flowability. However, given the different manufacturing conditions, relying solely on experimental assessments of powder flowability is insufficient to characterise the powder bed layer quality. Modelling and numerical simulation are ideal components for understanding the associated physical phenomena at various scales while providing additional information that is difficult to obtain experimentally.

The powder bed is a discrete domain; the discrete element method is ideal for simulating the complex particle behaviour during the spreading process. For instance, using DEM modelling, Yim et al. [3] has concluded that the predominant factor governing properties of the powder bed is the particle size distribution rather than particle sphericity. Several researchers have attempted to study powder flowability to optimise the spreading process; Ma et al. [4] demonstrated that a high count of fine particle fractions produces superior powder bed quality in terms of the smooth finished surface and high mass density. However, on the other hand, an excessive fine fraction in the powder bed will cause major flowability issues.

The accuracy of any DEM model depends on the input values assigned to the parameters as determined through a calibration process [1]. For this reason, Dai et al. [5] attempted to study powder flowability using DEM simulation validated by an experimental assessment. Using the revolution powder analyser, they have shown that the rolling motion of non-spherical powders was the cause of an instantaneous disturbance to the flow of neighbouring powder particles. Others studied flowability by simulating a Hall flow meter, another flowability characterisation experimental technique. Through similar work, Phua et al. [6] calibrated their DEM model for Hall flow simulation using an experimental angle of repose and mass-flow rate measurements.

Similarly, this research uses a scaled Hall flow meter geometry and DEM computation to study metal powders at the microscale, emphasising the flowability of the AM powder bed. To calibrate the relative DEM metal powder model parameters for the stainless steel 316L metal alloy, it combines DEM simulations of the Hall flow meter characterisation technique with in-situ experimental data. We may acquire a thorough grasp of the effects DEM parameters have on simulated powder flow behaviour using the model created in this study, as well as extract suitable friction coefficients for the appropriate powder flow properties commonly employed in powder-bed spreading DEM models.

2. Materials and methods

This work investigates the flowability of gas-atomized stainless steel 316L metal alloy powder, and its particle size distribution, given in Figure 1, was measured using the CAMSIZER X2 Video-Granulometer. The chemical composition is given in Table 1.

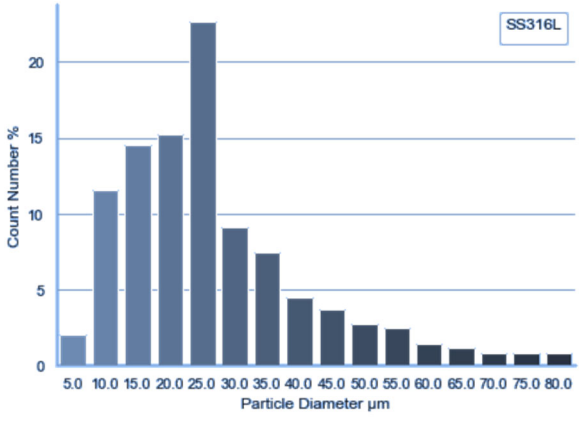

Fig. 1. Particle size distribution (PSD)

Table 1.
SS316L Chemical composition

Virgin SS316L, wt.%								
Fe	Ni	Cr	Si	Mn	Mo	O	P	C
balance	12.92	18.43	0.94	1.94	2.46	1.42	0.04	0.03

2.1. Discrete element method

Discrete element method DEM is a Lagrangian-based method able to model with high-fidelity the granular materials. An approach capable of modelling small particle interactions, after which their subsequent motion is computed using initial conditions, contact models, and other forces such as $\vec{F}_i^{wall}$ forces applied by surrounding walls, $\vec{F}_i^{bond}$ particle bonds, drag $\vec{F}_i^{drag}$ and $\vec{F}_i^{em}$ electromagnetic forces as shown in the equation (1).

$$m_i \ddot{r}_i = \vec{F}_i^{Contact} + \vec{F}_i^{wall} + \vec{F}_i^{bond} + \vec{F}_i^{drag} + \vec{F}_i^{em} \quad (1)$$

$$\vec{F}_{ij}^{Contact} = \mathcal{F}\left(\|r_i - r_j\|, R_i, R_j, \text{material parameters}\right) \quad (2)$$

where m_i and r_i are respectively the mass and position vector for each i^{th} particle. R_i, R_j are two radiuses of two particles **i** and **j**, the contact between these particles is activated when $\|r_i - r_j\| \leq R_i + R_j$.

The particle contact mechanics used in this work capture normal F_{ij}^n, tangential F_{ij}^t and angular contact related to normal interactions and angular velocity between particles, which helps establish a directional torque proportional to the normal contact force [7].

$$F_{ij}^n = \left(k_n \delta_n - \gamma_n V_{n,ij}\right) n_{ij}\,, \quad F_{ij}^t = \left(k_t \delta_t - \gamma_t V_{t,ij}\right) t_{ij} \quad (3)$$

where $\delta_n n_{ij}$ and $\delta_t t_{ij}$ are, respectively, the normal and tangential overlap. Also, $V_{n,ij} n_{ij}$ and $V_{t,ij} t_{ij}$ are, respectively, normal and tangential relative velocity. k_n, k_t, γ_n and γ_t are model coefficients computed based on Young and shear modulus, respectively. The particle-particle and particle-wall interaction forces were calculated using a Hertzian contact model without cohesiveness. This work considers gravity's forces and torques, collisions, and sliding and rolling friction. The governing equations were solved using the open-source LIGGGHTS framework [8].

2.2. Metallic powder characterization method

The flowability is not an inherent property of metal powder because it is affected not only by the powder's physical properties (shape, particle size, humidity, etc.) but also by the characterization apparatus and relative measurement method used, namely the Hall flow meter [9], revolution powder analyser [5] and shear cell test [10]. The funnel geometry of the Hall flow meter is based on the specification of the ASTM B213-17.

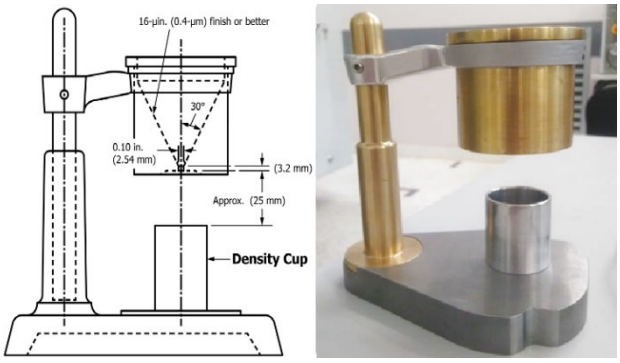

Fig. 2. Experimental Hall flow meter

The apparatus used in the experiment is shown in Figure 2. The funnel is a 30° cone with an orifice of 2.45 mm. The test involves recording the time for 50 grams of powder to flow through the funnel, known as the Hall flow value. Additionally, we measure the angle of the pile of powder at the end of the funnel flow, referred to as the angle of repose.

2.3. Simulation step-up

This model simulates a highly spherical SS316L stainless steel alloy. The parameters used in our DEM model are shown in Table 2. The modelled morphology is spherical, and the particle size distribution was converted from a volume-based distribution to a number-based distribution (as shown in Fig. 1), which was used to create the initial particle cloud.

Table 2.
SS316L powder model parameters for DEM simulation

Material properties			
Young modulus, GPa	208	Rolling friction	0.2-0.5
Density, kg/m^3	7980	Sliding friction	0.3-0.5
Poisson ratio	0.267	Coefficient of restitution	0.3
Cumulative volume, % [D_{10}, D_{50}, D_{90}]	8, 22, 45	Time step, s	10^{-6}

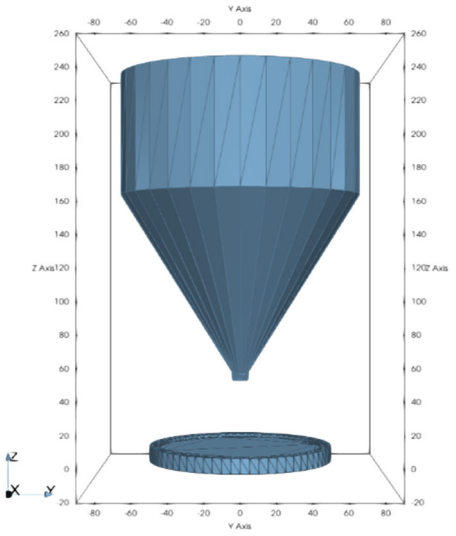

Fig. 3. Simulation domain for virtual Hall flow meter

The simulated particles are only affected by gravity, while drag forces from the surrounding air are not consider. The sliding and rolling friction coefficients varied between 0.1 and 0.5 to find parameter values corresponding to the experimental Angle of Repose (AOR). However, this alone is not sufficient to model flowability, which is why a mass flow assessment is also needed to select the appropriate parameters that match both AOR and mass flow.

The simulations were run in parallel using 20 CPUs on an Intel Xeon workstation. The present model simulates 30 k particles with a 10^{-6} time step. The convergence criterion considered both Rayleigh and Hertz Time Limit [11].

Additionally, the computational power needed to model full scale is a significant limitation for modelling metal powder particles using DEM. To compensate for the increased particle size, the funnel geometry in our simulation domain was scaled down using a modified Beverloo law [12] given by Equation (4); this law accurately estimates the mass flow rate through the scaled-down orifice.

$$Q = C\rho g^{1/2}(D - kd)^{5/2} \quad (4)$$

where D is the orifice size, d is the mean diameter of the particles, g is the gravity constant, and k is the dimensionless constant be 1 and 2. At the same time, C is the dimensionless flowability constant. Our model utilized two scaling factors, scaling up the particles by a factor of 10^3 and scaling down the geometry by a factor of 10^2.

3. Results and discussion

ParaView has been used for rendering the virtual Hall flow meter and Python for data analysis. As seen in Figure 4, this simulation comprises three steps: cloud generation, free fall and funnel flow at the orifice (D_0 = 2.45 mm). The first two steps, Cloud generation and free fall step are where the powder settles at the base of the funnel under less than 1 s. This model uses sliding friction SF and rolling friction RF. Instead of using cohesive forces, a constant directional torque (CDT) was added to the modelled particles.

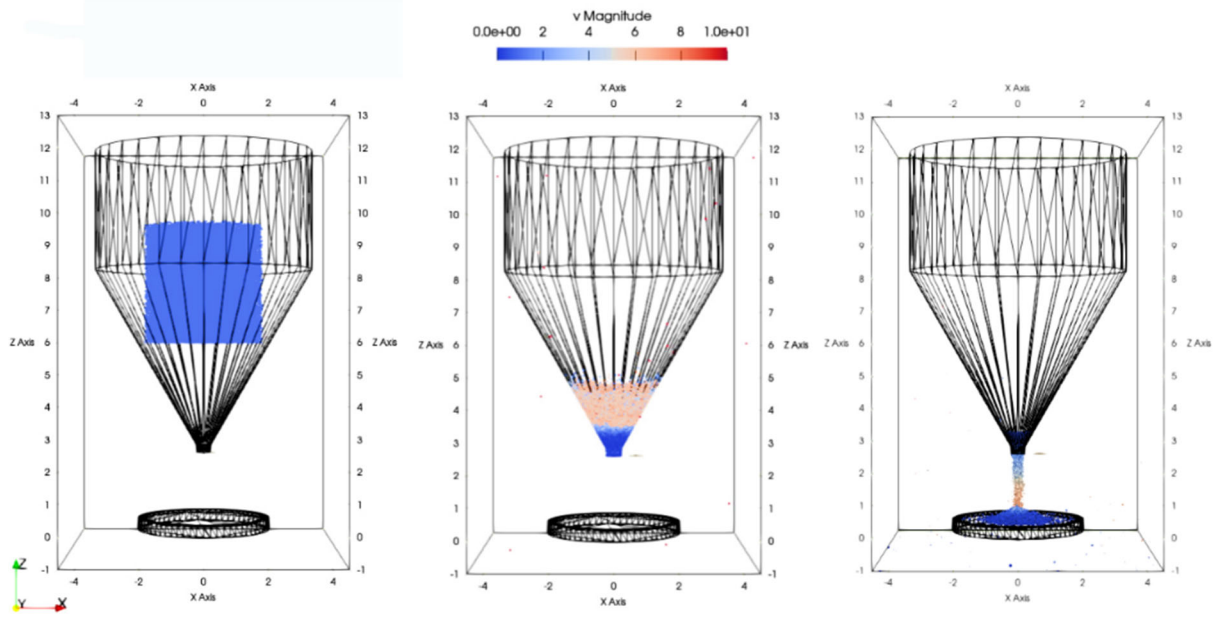

Fig. 4. Simulation steps cloud generation, free fall and funnel flow (left to the right)

The Constant Directional Torque (CDT) is the most commonly used in DEM research owing to its relatively accurate and efficient calculations. In this model, the resistive torque τ_r is proportional to the normal force F_{ij}^n and is oriented in the direction of the relative rolling motion $\frac{\omega_{ij}}{|\omega_{ij}|}$. It is expressed as follows:

$$\tau_{ij}^r = -\mu_r R_{ij}{}^* \left|F_{ij}^n\right| \frac{\omega_{ij}}{|\omega_{ij}|} \quad (5)$$

The computed results acquired are velocity magnitude, forces and angular velocity presented in (Fig. 5). Depending on sliding friction at the orifice, the modelled particles interact with the funnel wall, decreasing their velocity.

At the end of the funnel flow step, the simulation particle forms a heap where the angle of repose is measured. The particles exhibit a maximum 6 m.s^{-1} velocity before hitting the top of the heap. Similarly, the maximum angular velocity is recorded at the top part of the powder heap, suggesting that the particles travel in a rolling motion rather than sliding. This will reflect on the simulated friction coefficients. As for the computed forces, particles with bigger sizes tend to record greater force magnitudes.

Simulated AOR measurements were taken for each rolling and sliding fiction combination presented in Table 2. The lower and upper limits for these measurements are presented in Figure 6.

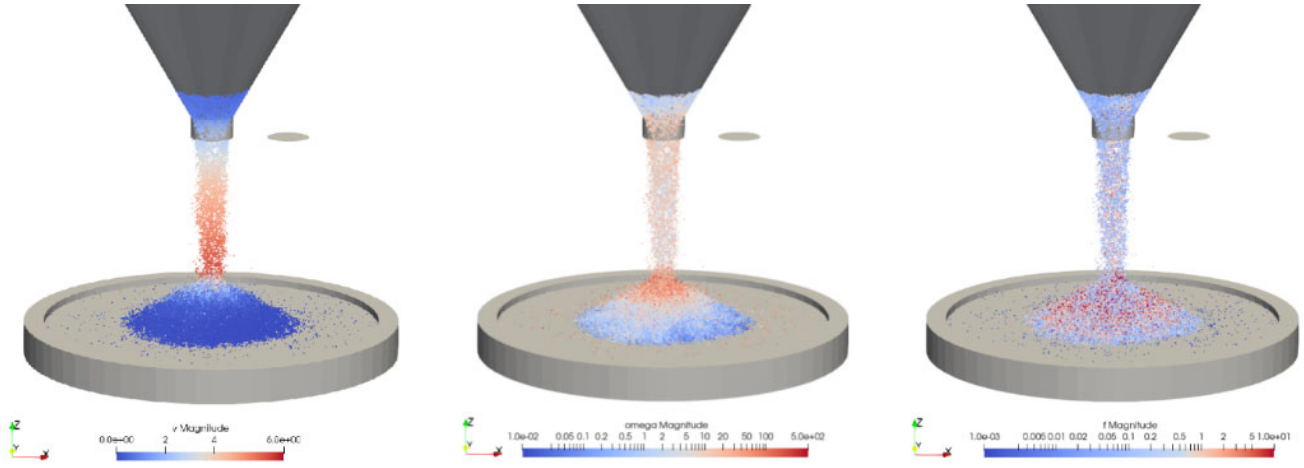

Fig. 5. Particle velocity (m/s), omega the, angular velocity (rad/s) and contact forces magnitude (N)

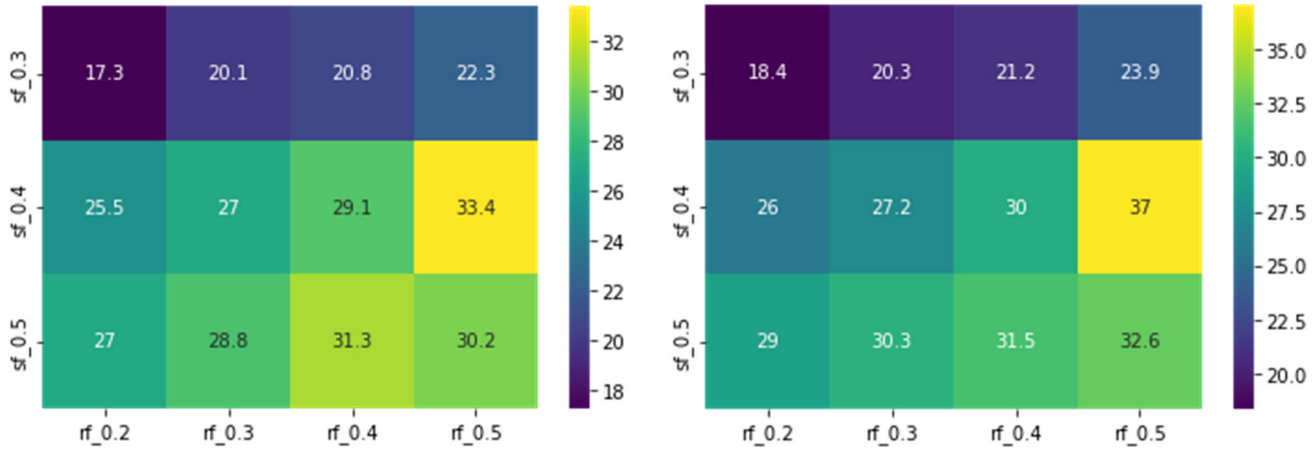

Fig. 6. A heatmap of simulated powder's AOR (lower value on the left and upper value on the right) with the used rolling and sliding friction coefficients

In the work of Du et al. [13], four different types of particle size distributions for SS316L powders were measured using the Hall flow meter. A PSD with more fine particles exhibits a lower powder flowability than a coarse particle distribution. This is reflected in both the mass flow (0.27 g/s) for coarse and 0.58g/s for fine-sized powder, and angle of repose 29.5° for coarse and 32.0° for fine-sized. As we have modelled a fine-sized particle distribution of SS316L, these results helped to establish the sliding and rolling coefficients needed to carry out DEM in the model parameters. Different combination of sliding and rolling frictions can sometimes result in similar AOR values. Furthermore, static AOR alone cannot reflect the actual flowability of the powder.

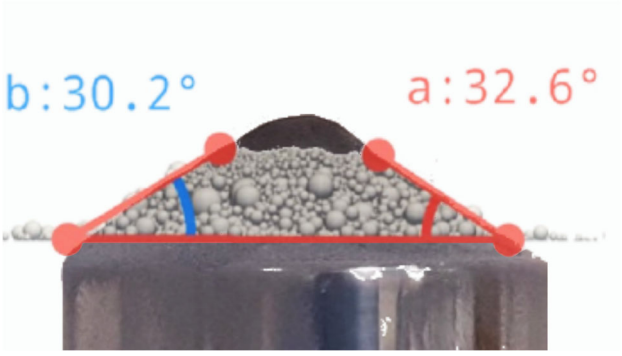

Fig. 7. Simulated powder's AOR acquired by our DEM model (in grey) superimposed to experimental powder heap

Therefore, to find the model parameters that best describe the flowability of the simulated powder, the simulation needs to generate a similar mass flow at the orifice (Hall value) taken by in situ measurements in combination with experimental AOR, using the specific sliding and rolling friction. As seen in Figure 7, the simulated AOR is between 30.2° and 32.6° acquired for 0.5 rolling resistance and 0.5 sliding resistance.

For this SS316L metal powder model, the best result was found at 0.5 SF and 0.5 RF. Figure 8 present simulation flow measurement. The simulated data taken at the orifice of the 3D funnel at 10^{-3} s resolution are the total mass passed through the orifice, the number of particles and their respective flow rates, the mass flow rate and particle number per unit of time. As seen in Figure 8C, the flow regime ends at 4.378 s, where all the simulated 30 k particles have fully left the funnel geometry. At that time, 2.5 g of mass had exited the orifice, as seen in Figure 8A. This computes to a mean mass flow rate of 0.571 g/s, validated by the real Hall flow value of 29.03s/50g for the desired AOR acquired experimentally. Moreover, 30 k particles is a relatively low number compared to other studies. This is attributed to using the Beverloo law to design the virtual Hall flow, allowing us to accurately simulate the particles' flow behaviour by modelling only 5% of the mass while achieving an accurate mass flow rate.

In contrast to other work like in Dai et al. [14], they used 400 k particles for full funnel geometry without considering the Beverloo law 32CPUs, their simulation of 400 k particles

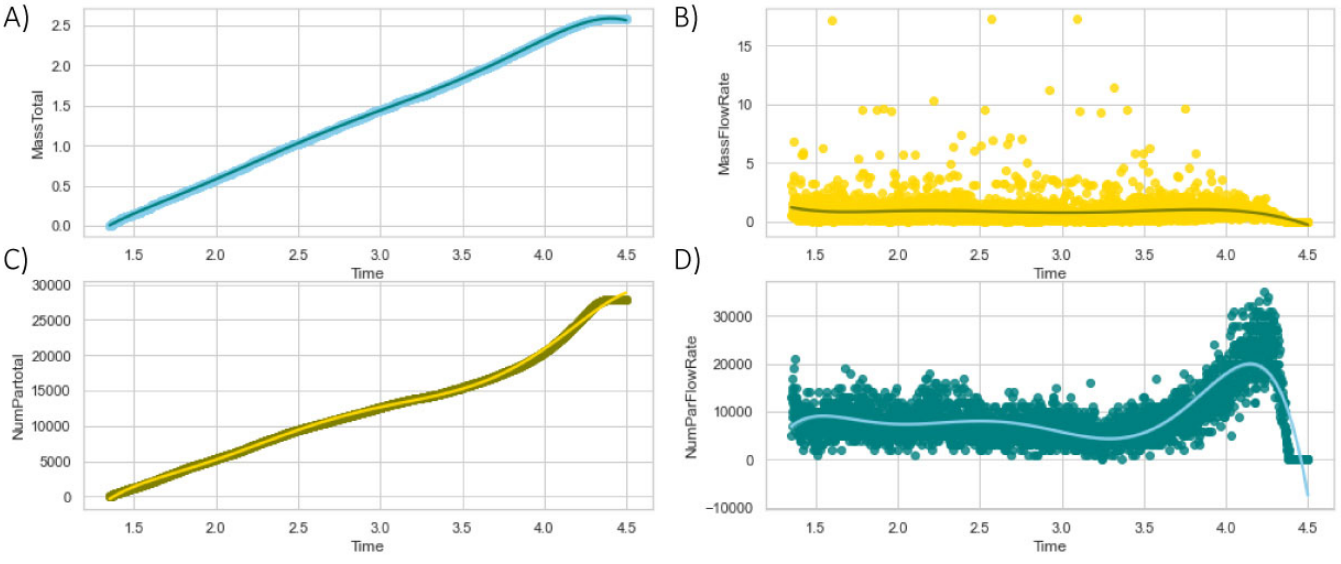

Fig. 8. The flow measurements at the orifice as a function of time. A) Total simulated mass exited the orifice, B) Simulated mass flow (yellow scatter), C) Total particles number exited the orifice, D) Particle number flow rate (green scatter)

took 14 days and 1 day of simulation time after scaling down to 50 k particles. The simulation in this work proved to run faster with only 6 hours with 20 CPUs; this is where CDT contact models overperform cohesive-based models by requiring less computing power. Additionally, we can notice in the number of particles in Figure 8D an oscillating behaviour where a peak is recorded before tailing off to zero. This peak is attributed to the large number of small-sized particles lagging due to the small travel distance in each contact iteration.

By examining results for the different simulations of friction parameters, we can notice that if rolling friction increases, the simulated Angle of repose is increased. As for mass flow rate, rolling friction effects were not so drastic. Conversely, the sliding friction decreases the mass flow rate drastically when increased, and along with it an increase in the angle of repose.

Other parameters like Young modulus and restitution coefficients had no effect on the modelled particles' bulk flow. However, the execution time increases drastically for higher values and the simulation diverges as Rayleigh and Hertz Time values are well above 20%. Therefore, a shorter time step is required, and the maximum number of simulated particles should be constrained to reach iterative convergence while keeping computational time at a minimum.

4. Conclusions

The virtual powder parameters (e.g., PSD, friction coefficients) inferred from the powder's intrinsic physical properties taken by in-situ measurements were enough to simulate metal powder particles flow behaviour; this strategy can further be improved with assessing the shape influence on flowability. The approach using DEM modelling, CDT contact model, and Beverloo Law for scaling geometry helped to model the flowability of metal powder on a micro-scale through a virtual static characterisation technique. This was validated by the simulated mass flow rate while matching the appropriate angle of repose obtained experimentally.

This study simulated 30 k particles, a relatively low number compared to other studies. The lower number was achieved by using the Beverloo law, which accurately simulated the particles' flow behaviour by modelling only 5% of the mass, which greatly reduced computation time.

In order to incorporate an experimentally validated particle flow behaviour, researchers investigating powder bed spreading can use the appropriate DEM parameters and coefficients found in this work, allowing them to study the effects of the spreading process for a similar SS316L metal alloy on a microscale (e.g. powder segregation, bed density, and recoating speed). Moreover, this approach can be replicated for other different materials, having different particle size distributions while considering the effects for different morphologies.

References

[1] A. Bouabbou, S. Vaudreuil, Understanding laser-metal interaction in selective laser melting additive manufacturing through numerical modelling and simulation: a review, Virtual and Physical Prototyping 17/3 (2022) 543-562. DOI: https://doi.org/10.1080/17452759.2022.2052488

[2] K. Riener, N. Albrecht, S. Ziegelmeier, R. Ramakrishnan, L. Haferkamp, A.B. Spierings, G.J. Leichtfried, Influence of particle size distribution and morphology on the properties of the powder feedstock as well as of AlSi10Mg parts produced by laser powder bed fusion (LPBF), Additive Manufacturing 34 (2020) 101286. DOI: https://doi.org/10.1016/j.addma.2020.101286

[3] S. Yim, H. Bian, K. Aoyagi, K. Yamanaka, A. Chiba, Spreading behavior of Ti-48Al-2Cr-2Nb powders in powder bed fusion additive manufacturing process: Experimental and discrete element method study, Additive Manufacturing 49 (2022) 102489. DOI: https://doi.org/10.1016/j.addma.2021.102489

[4] Y. Ma, T. M. Evans, N. Philips, N. Cunningham, Numerical simulation of the effect of fine fraction on the flowability of powders in additive manufacturing, Powder Technology 360 (2020) 608-621. DOI: https://doi.org/10.1016/j.powtec.2019.10.041

[5] L. Dai, Y.R. Chan, G. Vastola, Y.W. Zhang, Discrete element simulation of powder flow in revolution powder analyser: Effects of shape factor, friction and adhesion, Powder Technology 408 (2022) 117790. DOI: https://doi.org/10.1016/j.powtec.2022.117790

[6] A. Phua, C. Doblin, P. Owen, C.H.J. Davies, G.W. Delaney, The effect of recoater geometry and speed on granular convection and size segregation in powder bed fusion, Powder Technology 394 (2021) 632-644. DOI: https://doi.org/10.1016/j.powtec.2021.08.058

[7] A. Angus, L.A.A. Yahia, R. Maione, M. Khala, C. Hare, A. Ozel, R. Ocone, Calibrating friction coefficients in discrete element method simulations with shear-cell experiments, Powder Technology 372 (2020) 290-304. DOI: https://doi.org/10.1016/j.powtec.2020.05.079

[8] C. Kloss and C. Goniva, LIGGGHTS – Open Source Discrete Element Simulations of Granular Materials

Based on Lammps, in: TMS (eds), Supplemental Proceedings: Materials Fabrication, Properties, Characterization, and Modeling, John Wiley & Sons, Hoboken, 2011, 781-788.
DOI: https://doi.org/10.1002/9781118062142.ch94

[9] ASTM B213-17. Test Methods for Flow Rate of Metal Powders Using the Hall Flowmeter Funnel, ASTM, 2020. DOI: https://doi.org/10.1520/B0213-17

[10] J. Zegzulka, D. Gelnar, L. Jezerska, R. Prokes, J. Rozbroj, Characterization and flowability methods for metal powders, Scientific Reports 10 (2020) 21004. DOI: https://doi.org/10.1038/s41598-020-77974-3

[11] S.J. Burns, P.T. Piiroinen, K.J. Hanley, Critical time step for DEM simulations of dynamic systems using a Hertzian contact model, International Journal for Numerical Methods in Engineering 119/5 (2019) 432-451. DOI: https://doi.org/10.1002/nme.6056

[12] C. Mankoc, A. Janda, R. Arévalo, J.M. Pastor, I. Zuriguel, A. Garcimartín, D. Maza, The flow rate of granular materials through an orifice, Granular Matter 9/6 (2007) 407-414.
DOI: https://doi.org/10.1007/s10035-007-0062-2

[13] K. Du, S. Li, S. Jie, X. Gao, Y. Yu, Effect of 316L stainless steel powder size distribution on selective laser melting process, Journal of Physics: Conference Series 1347 (2019) 012121.
DOI: https://doi.org/10.1088/1742-6596/1347/1/012121

[14] L. Dai, Y. R. Chan, G. Vastola, N. Khan, S. Raghavan, Y.W. Zhang, Characterizing the intrinsic properties of powder – A combined discrete element analysis and Hall flowmeter testing study, Advanced Powder Technology 32/1 (2021) 80-87.
DOI: https://doi.org/10.1016/j.apt.2020.11.015